

**Endotaxial Si nanolines in Si(001):H**

F. Bianco, J. H. G. Owen, S. A. Köster, D. Mazur, and Ch. Renner\*

*Department of Condensed Matter Physics, NCCR MaNEP, University of Geneva, 24 Quai Ernest-Ansermet, CH-1211 Geneva 4, Switzerland*

D. R. Bowler

*Department of Physics & Astronomy, University College London, Gower St, London WC1E 6BT, United Kingdom London Centre for Nanotechnology, 17–19 Gordon St, London WC1H 0AH, United Kingdom*

(Received 16 March 2011; published 29 July 2011)

We present a detailed study of the structural and electronic properties of a self-assembled silicon nanoline embedded in the H-terminated silicon (001) surface, known as the Haiku stripe. The nanoline is a perfectly straight and defect-free endotaxial structure of huge aspect ratio; it can grow micrometer long at a constant width of exactly four Si dimers (1.54 nm). Another remarkable property is its capacity to be exposed to air without suffering any degradation. The nanoline grows independently of any step edges at tunable densities from isolated nanolines to a dense array of nanolines. In addition to these unique structural characteristics, scanning tunneling microscopy and density functional theory reveal a one-dimensional state confined along the Haiku core. This nanoline is a promising candidate for the long-sought-after electronic solid-state one-dimensional model system to explore the fascinating quantum properties emerging in such reduced dimensionality.

DOI: [10.1103/PhysRevB.84.035328](https://doi.org/10.1103/PhysRevB.84.035328)

PACS number(s): 81.07.Gf, 68.65.-k, 73.21.Hb, 81.16.Dn

**I. INTRODUCTION**

There is tremendous scientific and technological interest in physical systems of reduced dimensionality.<sup>1</sup> Nanowires down to single-atom chains are of particular interest. The Fermi-liquid theory describing conventional bulk conductors breaks down in such one-dimensional (1D) systems, which are predicted to behave remarkably differently. The concept of a single particle becomes obsolete and one has to switch to a description of collective spin and charge excitation.<sup>2</sup> However, the unusual properties of the non-Fermi liquid counterpart, the Tomonaga-Luttinger liquid,<sup>3</sup> remain largely untested by experiment due to the lack of suitable practical models for electronic systems.

The experimental quest for exotic quantum phenomena in reduced dimensions such as quantized conductance,<sup>4</sup> charge density waves,<sup>5</sup> Wigner crystals,<sup>6</sup> Peierls distortions,<sup>7</sup> and spin-charge separation<sup>8</sup> has triggered numerous developments in the fabrication of nanostructures over the last decade.<sup>9,10</sup> Optical and electron-beam lithography as well as nanoimprint techniques all suffer from physical limitations and low fidelity on nanometer length scales. Scanning probes enable the fabrication of nanostructures down to single-atom assemblies.<sup>11–13</sup> However, this is a tedious and not scalable procedure limited to assemblies of few tens of atoms only. Moreover, their properties correspond to a particle in a box and are not suitable to probe, for example, transport in 1D.

A very attractive alternative capable of producing single-atom scale structures in a very efficient and scalable manner is self-assembly. Semiconductor surfaces, especially silicon, are among the favorite substrates to self-assemble nanowires. This is motivated by their compatibility with the current industrial information-technology processing<sup>14</sup> and with state-of-the-art nanoscale processing techniques.<sup>15</sup> Another reason is the energy gap at the Fermi level allowing to decouple the nanowire and substrate electronic states, which is paramount to obtaining 1D isolated nanowires on a bulk substrate. A range of metal atoms have been self-assembled into atomic chains

on vicinal Si(553) and Si(557) surfaces,<sup>16,17</sup> and on Si(111) and Ge(001) terraces.<sup>18,19</sup> In the first instance, the nanolines assemble along the step edges, hence their spacing (density) is set by the vicinal angle. In the second instance, the nanolines form a dense array. The metallic rare-earth silicides comprise another interesting family of 1D systems that has been a focus of attention for many years.<sup>20</sup> Their 1D growth is due to anisotropic epitaxial strain induced by unidirectional lattice mismatch.<sup>1</sup> YSi<sub>2</sub> nanowires have been found to exhibit 1D states.<sup>21</sup> However, the major shortcoming of these structures is their nonconstant width and their high reactivity with air.

Here, we present a novel and very promising self-assembled silicon only nanoline structure embedded in the flat terraces of Si(001). These endotaxial (i.e., epitaxially grown *into* the substrate<sup>22</sup>) nanolines, obtained through hydrogenation of precursor Bi nanolines,<sup>20,23</sup> exhibit a range of remarkable properties. Like other endotaxial structures in Si(001), such as silicide nanowires,<sup>24</sup> they show large aspect ratios with lengths that can exceed 1 μm. Moreover, they offer striking advantages over all other nanolines mentioned above: they are absolutely straight at a constant width of exactly four Si dimers (1.54 nm), they are atomically perfect and nearly defect free, they are stable upon air exposure for at least 25 minutes, they grow on the flat terrace away from any step edges, and their density can be tuned from isolated and noninteracting nanolines to dense arrays of possibly interacting nanolines.

We shall first describe the fabrication of these endotaxial Si nanolines. Then, we discuss their structural and electronic properties in detail based on experimental data from scanning tunneling microscopy (STM), x-ray photoelectron spectroscopy (XPS), reflection high-energy electron diffraction (RHEED), and density-functional-theory (DFT) modeling.

**II. METHODS**

Endotaxial Si nanolines on Si(001) were fabricated and studied in ultrahigh vacuum (UHV—base pressure in the low

$10^{-11}$  mbar) using an Omicron low-temperature STM. The sample preparation chamber is equipped with hot and cold stages to control the substrate temperature during nanoline growth, several Knudsen cells, electron-beam-evaporation sources, a high-efficiency hydrogen cracker, and an ion gun. The nanowire growth is monitored in real time using RHEED, and we further utilize XPS for chemical characterization.

Boron-doped *p*-type Si(001) substrates with a resistivity of  $0.1 \Omega \text{ cm}$  were prepared using a standard *ex-situ* and *in-situ* cleaning sequence. *Ex-situ* cleaning starts with degreasing the substrates in ultrasonic acetone followed by isopropanol baths for 5 minutes each. Each substrate is then rinsed in purified water and cleaned in an oxidizing mixture of  $\text{H}_2\text{O}_2$  and  $\text{H}_2\text{SO}_4$  (1 : 1 by volume) for 30 seconds. This surface oxide is subsequently removed by a 30-second HF (15 wt%) dip. Finally, the above oxidation step is repeated to regrow a thin protective oxide film and the substrate is rinsed in purified water and dried with nitrogen gas. *In-situ* cleaning starts by degassing the Si(001) substrate for typically 12 hours at  $600^\circ\text{C}$  while keeping the pressure below  $1 \times 10^{-9}$  mbar. To obtain a clean surface, it is then repeatedly flash-annealed at  $1200^\circ\text{C}$  while making sure the pressure is kept below  $2 \times 10^{-9}$  mbar. This step is repeated until the substrate can be flashed-annealed for 10–15 s. The last flash-annealing is followed by a controlled cool-down from  $900^\circ\text{C}$  to the nanowire growth temperature of  $570^\circ\text{C}$  in roughly 1 minute.

To obtain the precursor nanolines [see Fig. 1(a)], bismuth is evaporated for 10 to 15 minutes onto the clean Si(001) surface kept at  $570^\circ\text{C}$  from a MBE Komponenten K-cell heated to  $470^\circ\text{C}$ . After the deposition, the sample is kept at  $570^\circ\text{C}$  for 2 to 3 additional minutes, and then cooled down to the hydrogenation temperature of  $300^\circ\text{C}$ . The entire deposition process is monitored in real time with RHEED. The characteristic arc in the RHEED pattern [see Fig. 1(b)] signaling the formation of Bi nanolines appears 6 to 8 minutes into the deposition process.

The Bi nanolines thus obtained are exposed to a hydrogen atomic beam from a MBE Komponenten HABS high-efficiency hydrogen cracker heated to  $1600^\circ\text{C}$ .<sup>25</sup> The sample temperature is set at  $300^\circ\text{C}$  during the hydrogenation process. Hydrogen is fed into the UHV chamber through the cracker itself and the flow rate is controlled by maintaining a constant chamber pressure of  $2.5 \times 10^{-7}$  mbar. The Si(001) surface and the Bi nanolines are exposed to the atomic hydrogen flux for 4–8 minutes, corresponding to doses of 60–120 L. We found that this amount of hydrogen is sufficient to saturate all the Si dangling bonds to form a monohydride surface.<sup>26</sup> It also fully strips the bismuth off the surface, saturating the exposed Si bonds with hydrogen but without affecting the underlying one dimensional Haiku reconstruction.<sup>23</sup> This results in a 1D endotaxial hydrogen-saturated Si nanoline, called the Haiku stripe,<sup>23</sup> which is the subject of detailed investigations in the following sections.

We performed DFT<sup>27,28</sup> calculations using a plane-wave implementation within the generalized-gradient approximation (GGA). All calculations have been performed with the VIENNA *ab initio* simulation package (VASP).<sup>29,30</sup> Ultrasoft pseudopotentials<sup>31</sup> are used for all the elements considered. Convergence of forces and energy differences is achieved by

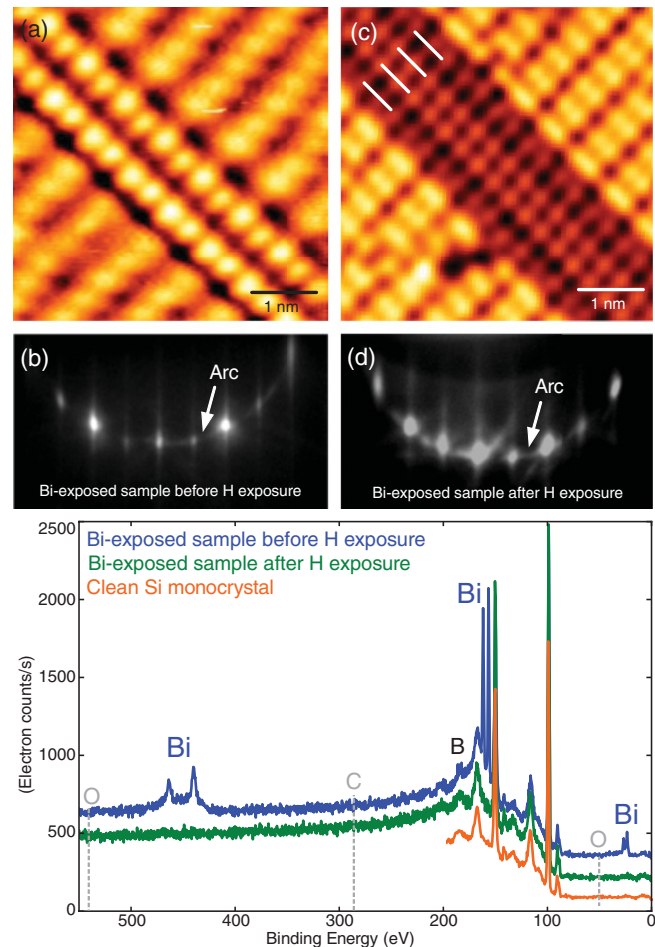


FIG. 1. (Color online) (a) High-resolution STM micrograph of a Bi nanoline on a clean Si(001) background. (Sample bias  $V = -3.5$  V,  $I = 200$  pA, and  $T = 77$  K) (b) RHEED pattern after Bi growth. The arc signifies the Bi nanoline and the bright dots are due to the  $2 \times 1$  reconstruction of the Si surface. (c) High-resolution STM micrograph of the Haiku stripe (4-Si-dimers-wide diagonal structure) revealed after the hydrogen-induced removal of the Bi atoms. ( $V = -2.8$  V,  $I = 200$  pA, and  $T = 77$  K) (d) RHEED pattern showing the characteristic arc of a well-ordered 1D structure on the surface, the Haiku stripe. (e) XPS spectra measured on the Si(001) surface at the different states of sample preparation. The small peak at 188 eV is due to B dopant atoms. No peaks from contamination of C or O are resolved. The top curves are offset by +100 and +200 counts/s for clarity.

selecting a Monkhorst-pack<sup>32</sup> mesh of  $4 \times 2 \times 1$  to sample the Brillouin zone and an energy cutoff of 200 eV. Energy differences are converged to within 0.01 eV and forces to  $0.02 \text{ eV}/\text{\AA}$ . We used a unit cell, which was one dimer row wide, ten dimers long, and ten layers deep with the bottom two layers fixed and the bottom layer terminated with hydrogen.<sup>33,34</sup> The commonly used scheme to simulate STM images is based on Tersoff-Hamann approximation, which asserts that the LDOS is proportional to the tunneling current. By assuming that the tip has a flat density of state, the STM simulations are then integral of all the partial charge density for the bands between the bias voltage and the Fermi level.

### III. RESULTS

#### A. Haiku stripes

While the Bi nanolines appear to STM as a pair of Bi surface dimers, there is a substantial reconstruction of the underlying Si lattice—a triangular core of Si embedded in the top five layers of the Si substrate called the Haiku core. The Bi nanolines, with the unique Haiku structure, have been found to be the lowest energy reconstruction of Si(001):Bi.<sup>35</sup> In DFT calculations, the Haiku structure is 0.36 eV/Bi dimer more favorable than the next best proposed structure<sup>35</sup> and 0.25 eV/Bi dimer more favourable than one monolayer of Bi.<sup>36</sup> A remarkable result of our work is to find that this structure remains stable in the hydrogenated Si(001) surface, despite the removal of the Bi dimers. Both the Bi nanoline [see Figs. 1(a) and 1(b)] and the Haiku stripe [see Figs. 1(c) and 1(d)] manifest themselves as an arc in the RHEED pattern measured along  $\langle 110 \rangle$ , a direct consequence of their 1D nature and direct evidence of the subsurface reconstructed core. Annealing experiments on Haiku stripes showed that the arc feature remains in RHEED up to a temperature of about 400 °C. This contrasts with previous experiments and simulations on burial of the nanolines by Si that found that the Haiku core structure is spontaneously dissociated during overgrowth by Si.<sup>37</sup> Figure 1(e) shows XPS spectra of the Bi-exposed surface before and after exposure to hydrogen. Characteristic Bi peaks at 464, 440, 157, 159, and 25 eV, which are clearly resolved after the Bi nanoline growth, completely disappear upon hydrogenation of the Si(001) surface. The XPS spectrum of the hydrogenated surface is indistinguishable from the pristine Si(001) surface. No contaminant species is detected except for a minute B signal originating from the bulk dopant atoms. STM micrographs provide further evidence that the Haiku stripe imaged in Fig. 1(c) is not just a different appearance of the Bi nanoline due to particular imaging conditions. The Haiku stripes appear dark independent of bias, which unquestionably distinguishes them from the Bi nanolines whose STM image contrast is always bright relative to a H-terminated surface.<sup>20</sup>

In Fig. 1(c), the STM micrograph of the hydrogen-covered-Haiku-core structure shows well-resolved dark stripes. The dark stripes observed after the Bi has been stripped off can be explained by a replacement of each Si-Bi bond pair by two Si-H bonds.<sup>23</sup> The proposed structure from DFT of the resulting H-saturated endotaxial Si nanoline is illustrated in the ball-and-stick model of Fig. 2. Its key feature is the Haiku core—a major reconstruction of the silicon extending five layers below the surface and composed of 5- and 7-fold Si rings. The four rows of dots indicated by short solid white lines in the STM micrograph of the Haiku stripe [see Fig. 1(c)] correspond to the four H atoms spanning the Haiku stripe over exactly 4 Si dimers (1.54 nm). These rows appear 60 to 70 pm deeper than the surrounding Si(001):H surface, in quantitative agreement with the value expected from the relaxed structure in the DFT simulation (see Fig. 2) and in good agreement with the depth of similar P-terminated 5-7-5 structures.<sup>38</sup>

The above result suggests that Bi can be fully stripped off from the Bi nanolines. This is opposite to previous experiments on hydrogenation of Bi nanolines, which have reported that the nanolines were inert,<sup>20</sup> except for a recent indication of

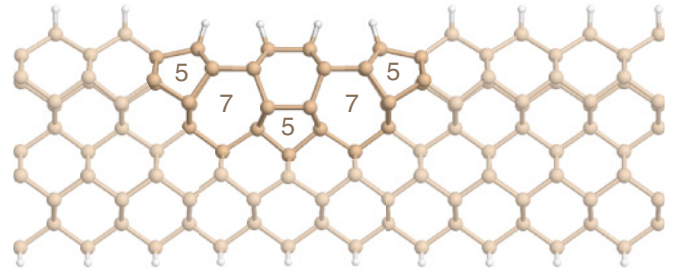


FIG. 2. (Color online) Ball-and-stick model of the DFT structure for the Haiku stripe showing the 5- and 7-fold ring reconstruction of the Haiku core (cross section).

Bi nanoline damage with a very large dose (1000 L H<sub>2</sub>) by Wang *et al.*<sup>39</sup> We explain this controversy on the basis of the different hydrogenation setups used. All the previous experiments were done using a hot filament, whereas we are using a high-efficiency hydrogen cracker. The geometry of the H-cracker exposes the sample to a much greater density of hot hydrogen accelerated toward the sample. The gas flux impacts the sample at an angle of 25°. By contrast, a hot filament sends the gas atoms and molecules in all directions, thus reducing the flux density. The exact mechanism by which H replaces the Bi atoms is not understood at present. One possibility is that hot uncracked H<sub>2</sub> molecules reach the surface with sufficient kinetic energy to attack the Bi-Si bonds, thus exposing Si dangling bonds, which are quickly capped by H atoms. To test this idea, we lowered the temperature of the H cracker, thus greatly reducing the flux of atomic hydrogen. We observed no reduction of the Bi nanoline stripping rate, suggesting that hot, high-kinetic-energy H<sub>2</sub> molecules hold the key to the observed stripping effect.

Since the Si(001) surface is very reactive to water, we took special care to reduce the exposure to impurity water. We carefully baked the gas line back to the H-bottle, and further cryopumped the hydrogen gas used in the gas line. In addition, we have used a dedicated cracker, degassed over many hours at operating temperature (1600 °C). The chamber pressure with the cracker at 1600 °C is  $8 \times 10^{-10}$  mbar. The cracker has a much higher efficiency than a hot filament.<sup>25</sup> This allows us to achieve a saturation H coverage with a very small amount of H<sub>2</sub> gas (60–120L), thereby greatly reducing the exposure to any impurities. To achieve saturation of the surface with a hot filament typically H<sub>2</sub> doses of 500–1000 L are required<sup>40</sup> (15–20 minutes exposure). In our case, any possible carbon or oxygen on the surface after atomic H dosing was below the XPS detection limit [see Fig. 1(e)]. Although we cannot measure the water partial pressure directly, we believe that any impurity water has been minimized and that any effect on the nanoline will come from the exposure to hydrogen.

Figure 3(a) shows a large-scale micrograph where many long stripes ( $>0.2 \mu\text{m}$ ) can be seen. The longest stripe on this STM micrograph, whose extremities are identified by black arrows in Figs. 3(a) and 3(b), reaches 1.3  $\mu\text{m}$ . The terrace containing this stripe is shown in more detail in Fig. 3(b). Figure 3(a) confirms that the Haiku stripes share a number

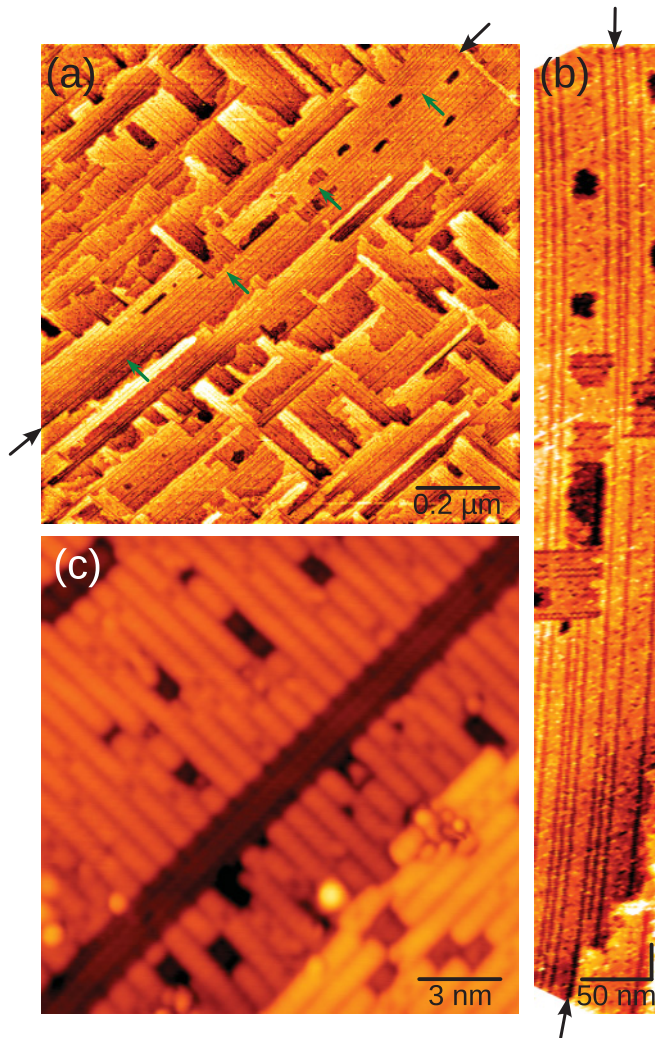


FIG. 3. (Color online) (a) STM image of long Haiku stripes. The black arrows denote the start and end points of a  $1.3\text{-}\mu\text{m}$ -long stripe, while the green arrows are guides for the eye. ( $V = -2.5\text{ V}$ ,  $I = 180\text{ pA}$ , and  $T = 77\text{ K}$ ) (b) Magnification of the  $1.3\text{-}\mu\text{m}$ -long stripe denoted by arrows in (a). For clarity, the horizontal axis has been stretched by a factor of two. (c) STM image taken after 25-min air exposure without any special treatment showing a Haiku stripe running diagonally through the image. Neither the surface nor the Haiku stripe have been attacked by reactants. The dark structures away from the stripe on the substrate, also present on as-grown surfaces, are either missing Si atoms or places where background Bi has been extracted by H. ( $V = -2.2\text{ V}$ ,  $I = 100\text{ pA}$ , and  $T = 77\text{ K}$ ).

of features with the Bi nanolines; they are straight without any kinks and have a fixed width, they are seen on terraces and terminate at defects and step edges. These properties have been attributed to the Haiku core. Additionally, the density of the Haiku stripes on the surface corresponds to the density of the precursor Bi nanolines and such stripes have never been seen after hydrogenation of the clean Si(001) surface. These facts substantiate our assumption that these lines result from hydrogenation of precursor Bi nanolines, and the Haiku core is the correct model for this endotaxial Si-in-Si(001) nanoline.

It has been known for many years that the Si(001) monohydride surface is stable in air for up to 40 hours.<sup>40</sup> Since the Si-H bond along the Haiku stripes is of similar strength as the usual Si-H bond on the hydrogenated Si(001) surface according to DFT, it is reasonable to expect air stability of the stripes. We checked this hypothesis experimentally, and Fig. 3(c) shows a Haiku stripe that is indeed still intact after 25 min exposure to air. The sample was transferred to the load lock, which was then slowly vented while the sample was protected from high-velocity molecules by lying at an angle pointing away from the leak valve as recommended by Ref. 40. Then the sample was stored in air for 25 min in a simple plastic box. After the exposure to air, the sample was reinserted into the load lock and transferred to the STM without any additional treatment.

The length of the Haiku stripes and their air stability offers a unique prospect to contact them to electrodes enabling standard transport experiments to be carried out. The air stability allows to consider common *ex-situ* semiconductor lithographic techniques unlike the precursor Bi nanolines or rare-earth silicide nanowires. In UHV, this can also be realized either by depositing metal on top of the surface using shadow-mask technology or by STM lithography using the H layer as a mask. Recent developments in the latter area<sup>41</sup> provide the ability to perform more complex contacting and gating of the stripes on a few-nm length scale.

## B. Electronic structure

STM is ideally suited to probe some of the quantum phenomena emerging in 1D systems, in particular, charge density waves, local spin phases, and van Hove singularities. Bias-dependent STM imaging is a very effective way to distinguish between purely electronic contrast due to, for example, localized states and structural contrast reflecting atomic positions. In the following, we compare topographic images measured at different sample bias voltages and tunneling current with DFT simulations. The experiment and model are in excellent agreement and reveal the existence of an extended 1D state at the surface along the Haiku core.

High-resolution STM micrographs reveal the Haiku stripe as a row of four dark atoms. In Fig. 4(a), recorded at a low current, they appear regularly spaced and all at the same elevation about  $70\text{ pm}$  lower (darker color) than the surrounding Si(001) surface. At a higher tunnelling current [see Fig. 4(b)], the middle two atomic sites appear raised by  $5\text{--}10\text{ pm}$  compared to the two outer atomic sites of the Haiku stripe. STM simulations [inset outlined by dashed rectangles in Figs. 4(a) and 4(b)] based on the DFT relaxed structure of the Haiku stripe (Fig. 2) perfectly reproduce all of the above characteristics. They were calculated for different tunneling currents at the same tunneling bias. Assigning specific current values to the STM simulations is challenging, and we are instead using selected values of integrated LDOS, which are high or low compared to the overall range of the data. Figure 2 shows that the four atomic sites spanning the Haiku stripe are physically at the same elevation, suggesting that the height contrast within the four-atoms-wide stripes is of purely electronic origin. The DFT simulation further reproduces very accurately the lateral position of the atomic sites with a clear

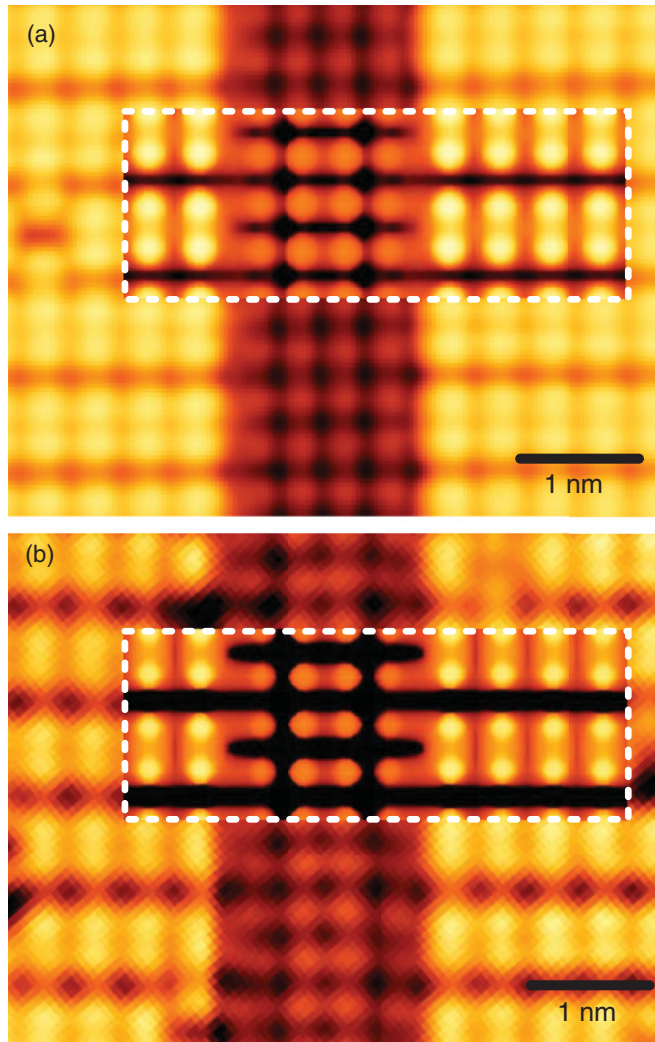


FIG. 4. (Color online) Filled-state high-resolution STM micrographs of the Haiku stripe with the corresponding DFT simulations shown within the dashed rectangles. (a) Sample bias  $V = -2.5$  V,  $I = 80$  pA, and  $T = 77$  K, DFT at  $-1.5$  eV for low current. (b)  $V = -2.8$  V,  $I = 200$  pA, and  $T = 77$  K, DFT at  $-1.5$  eV for high current.

shift of the two outer sites toward the edges of the Haiku stripe when observed at the higher tunneling current [see Fig. 4(b)].

Imaging the Si(001) at a positive tunneling bias, which probes the empty states of the sample, also reveals the four atomic sites across the Haiku stripe as shown in Fig. 5. The top half and the bottom half in panel (a) were taken one after the other with the same tip while only changing the bias magnitude. In contrast to the negative-bias images (see Fig. 4), the two central atoms along the Haiku stripe appear shifted away from each other, while the outer two are shifted toward the center of the structure (see Fig. 5). The central atoms now appear lower than the outer ones—the apparent height difference is reversed compared to the filled-state images. All these features illustrated in the magnified STM image sections [see Figs. 5(b) and 5(d)] are perfectly reproduced in the corresponding DFT simulations [see Figs. 5(c) and 5(e)].

The most remarkable feature in the empty-state STM images is a bright linear feature extending along the center of the Haiku stripe [see Fig. 5(a), top]. It is only seen in a narrow energy window around  $+2.0$  V, and does not match any atomic position in the Haiku model (see Fig. 2). Note that the background Si(001) is the same in the top and bottom sections of the micrograph shown in Fig. 5(a). Again, all these characteristics are perfectly reproduced by DFT; the simulation at  $+1.0$  V [see Fig. 5(c)] shows a linear electronic feature in the middle of the structure, whereas it is absent from the simulation at higher energy [see Fig. 5(e)].

In order to identify the origin of this 1D state, we computed the charge densities in the vicinity of a Haiku stripe. Figure 6 shows DFT isosurfaces of constant charge density for four bands starting at the conduction band minimum (CBM) toward higher energy states corresponding to the states probed primarily by STM at positive sample bias. The isosurfaces demonstrate the substantially different electronic structure below the surface of the Haiku core compared to pure Si. The first three bands above the lowest unoccupied molecular orbital (LUMO) show little to no charge density within the Haiku core and none of them are continuous along the stripes. On the other hand, the fourth band in Fig. 6(d) has its maximal charge density in the middle of the Si reconstruction. A cross section through the charge density along the center of the stripe [see Fig. 6(d), inset] shows that this fourth band is delocalized along the endotaxial nanoline, in excellent agreement with the STM observation [see Fig. 5(a), top].

### C. Discussion

The Haiku stripes are extremely-high-aspect-ratio Si-only 1D structures of unprecedented perfection. They offer a range of very attractive features toward the experimental exploration of 1D quantum physics. There is the experimental opportunity to attach contacts, which is paramount to the study of transport in a truly isolated 1D model system. The prime avenue will be the 1D state confined to the Haiku core but delocalized along it, which we have identified in STM and confirmed by DFT. One challenge will be to dope specifically the Haiku stripe. Local removal of the H atoms on the top of the stripe, followed by adsorption of  $\text{PH}_3$  (see Ref. 41) could lead to local doping of this state, for example. The physical and electronic structure of the stripes is well understood, so that experiments can enjoy strong theoretical support, while the micrometer length gives access to the infinite-length regime addressed by theory. Moreover, the degree of interaction between neighboring nanowires is tunable. Adjustable nanoline density is achieved by means of the growth temperature and Bi flux during the self-assembly of the Bi nanoline precursor. This is distinctly different from other self-assembled nanoscale wires, whose density can either not be adjusted<sup>42</sup> or is set by the step density of a vicinal surface.<sup>16</sup>

As well as the intrinsic properties of the Haiku stripes, they can also be used as a template for self assembling 1D chains of other atomic species. Previous experiments have shown templating properties for the Bi nanolines.<sup>43</sup> According to modeling, the stripes host favorable adsorption sites for a range of metal atoms. For example, Cu may diffuse into subsurface sites forming encapsulated single-atom chains.<sup>34</sup>

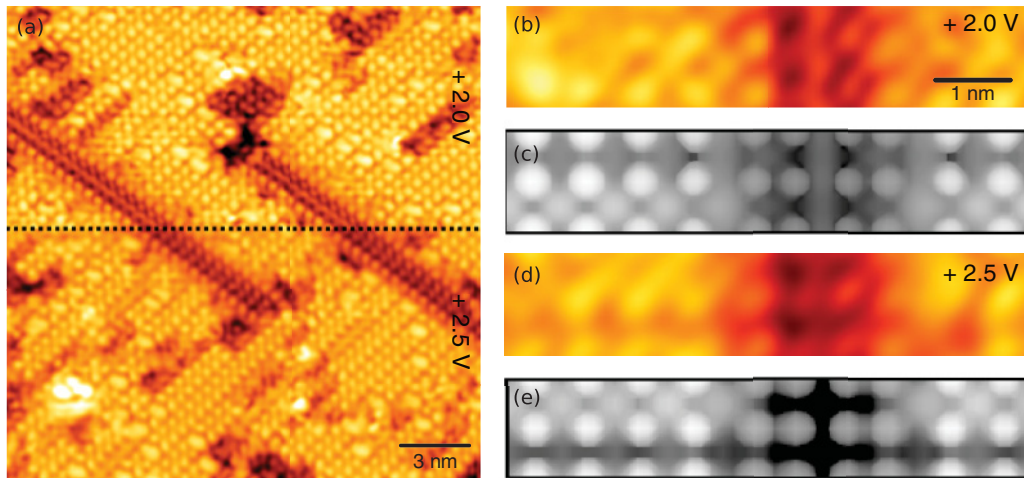


FIG. 5. (Color online) (a) Positive-sample-bias (empty states) STM micrographs of two Haiku stripes. Note the 1D state observed in the upper half of the image recorded at  $V = +2.0$  V, which disappears when the bias is increased to  $+2.5$  V in the lower half of the micrograph ( $I = 150$  pA,  $T = 77$  K). (b) A magnification of the central state of the Haiku stripe seen at  $V = +2.0$  V and (c) corresponding DFT model calculated for an energy of  $+1.0$  eV. (d) A magnification of the Haiku stripe at  $V = +2.5$  V and (e) the corresponding DFT model calculated for an energy of  $+2.5$  eV.

We are investigating the possibility that Mn atoms may also move into subsurface sites producing atomic chains with strong magnetic properties. The H-termination of the Haiku stripes offers the exciting possibility that such subsurface metal atomic chains would be stable in air.

Looking more broadly in the direction of future device fabrication, the H termination of these nanolines and consequent air stability, their micrometer length and their stability to an elevated temperature make these nanolines

compatible with a wide variety of semiconductor processing technologies.

#### IV. CONCLUSIONS

We have described the properties of a novel endotaxial Si nanoline in Si(001) identified as the Haiku stripe. Its core holds a delocalized state just above the conduction band minimum, which combined with the length and the perfection of the Haiku stripe makes it a very promising and

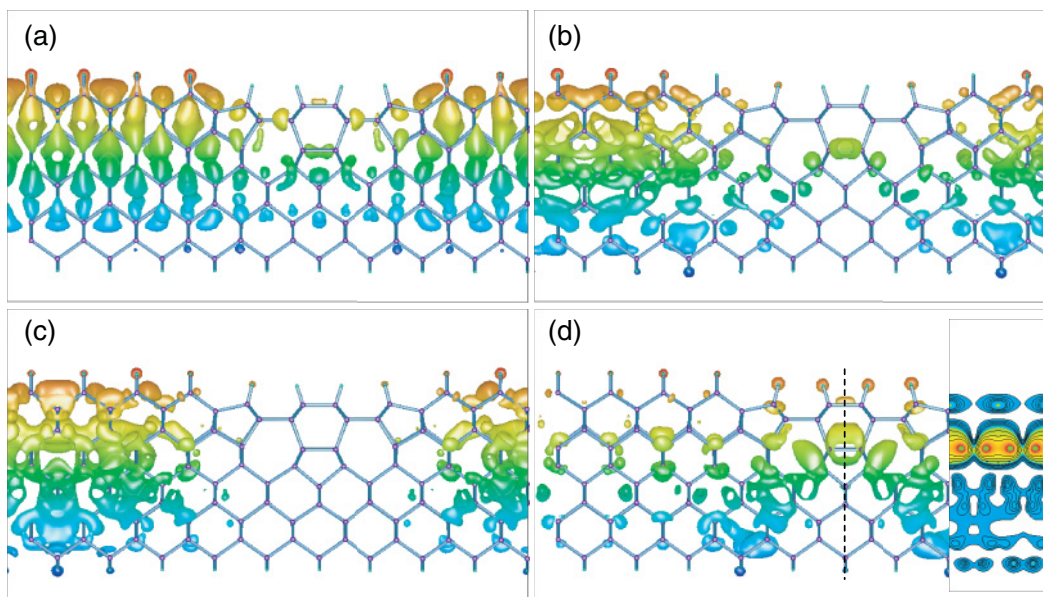


FIG. 6. (Color online) (a)–(d) Contour plots of constant-charge densities on the Haiku stripe cross section for the four bands above the conduction band minimum (CBM). The isosurface color represents the height within the structure. (a) The CBM, (b)  $+0.02$  eV, (c)  $+0.04$  eV, and (d)  $+0.10$  eV above the CBM. In (d), the charge density is located in the middle of the Haiku stripe. A cut through the charge density taken at the position of the dashed line reveals a delocalized state along the Haiku stripe. On the cut, the color corresponds to the charge densities: blue is a low density and red is a high-charge density.

appealing structure to explore quantum properties emerging in 1D. Moreover, the stability to air and to higher temperature, which we have demonstrated here, offer exciting experimental opportunities. The detailed matching of DFT simulations and STM micrographs confirms that the structure of the stripes is very well understood and settles the Haiku core model on firm ground. Thus the discovery of this unique Si-in-Si nanoline opens possibilities for exploring 1D physics and has a great potential for the fabrication of nanoscale electronic devices on a technologically relevant substrate.

## ACKNOWLEDGMENTS

The authors are very grateful to G. Manfrini for his expert technical support and to A. Rodriguez-Prieto for scientific discussions. We thank the Swiss National Science Foundation for financial support through the National Center of Competence in Research MaNEP (Materials with Novel Electronic Properties) and Division II. D.R. Bowler was supported by the Royal Society and acknowledges computational facilities in the London Centre for Nanotechnology.

\*christoph.renner@unige.ch

- <sup>1</sup>D. R. Bowler, *J. Phys. Condens. Matter* **16**, R721 (2004).
- <sup>2</sup>T. Giamarchi, *Quantum Physics in One Dimension*, (Oxford University Press, 2004) Chap. 2, 9, 10.
- <sup>3</sup>J. M. Luttinger, *J. Math. Phys.* **4**, 1154 (1963); D. C. Mattis, and E. H. Lieb, *ibid.* **6**, 304 (1965).
- <sup>4</sup>N. Agrait, A. Levy Yeyati, and J. van Ruitenbeek, *Phys. Rep.* **377**, 81 (2003).
- <sup>5</sup>G. Grüner, *Density Waves in Solids* (Addison-Wesley, Reading, MA, 1994).
- <sup>6</sup>H. J. Schulz, *Phys. Rev. Lett.* **71**, 1864 (1993).
- <sup>7</sup>S. Peierls and R. Peierls, *Quantum Theory of Solids* (Oxford University Press, USA, 2001).
- <sup>8</sup>M. G. Zacher, E. Arrighoni, W. Hanke, and J. R. Schrieffer, *Phys. Rev. B* **57**, 6370 (1998).
- <sup>9</sup>A. Nitzan and M. A. Ratner, *Science* **300**, 1384 (2003).
- <sup>10</sup>J. V. Barth, G. Costantini, and K. Kern, *Nature (London)* **437**, 671 (2005).
- <sup>11</sup>J. W. Lyding, T.-C. Shen, J. S. Hubacek, J. R. Tucker, and G. C. Abeln, *Appl. Phys. Lett.* **64**, 2010 (1994).
- <sup>12</sup>S. Fölsch, P. Hylgaard, R. Koch, and K. H. Ploog, *Phys. Rev. Lett.* **92**, 056803 (2004).
- <sup>13</sup>C. F. Hirjibehedin, C. P. Lutz, and A. J. Heinrich, *Science* **312**, 1021 (2006).
- <sup>14</sup>C. Teichert, *Phys. Rep.* **365**, 335 (2002).
- <sup>15</sup>F. J. Rueß, A. P. Micolich, W. Pok, K. E. J. Goh, A. R. Hamilton, and M. Y. Simmons, *Appl. Phys. Lett.* **92**, 052101 (2008).
- <sup>16</sup>F. J. Himpsel, J. L. McChesney, J. N. Crain, A. Kirakosian, V. Perez-Dieste, N. L. Abbott, Y.-Y. Luk, P. F. Nealey, and D. Y. Petrovykh, *J. Phys. Chem. B* **108**, 14484 (2004).
- <sup>17</sup>N. Oncel, *J. Phys. Condens. Matter* **20**, 393001 (2008).
- <sup>18</sup>J. Schäfer, C. Blumenstein, S. Meyer, M. Wisniewski, and R. Claessen, *Phys. Rev. Lett.* **101**, 236802 (2008).
- <sup>19</sup>J. Schäfer, S. Meyer, C. Blumenstein, K. Roensch, R. Claessen, S. Mietke, M. Klinke, T. Podlich, R. Matzdorf, A. A. Stekolnikov, S. Sauer, and F. Bechstedt, *New J. Phys.* **11**, 125011 (2009).
- <sup>20</sup>J. H. G. Owen, K. Miki, and D. R. Bowler, *J. Mater. Sci.* **41**, 4568 (2006).
- <sup>21</sup>C. Zeng, P. R. C. Kent, T.-H. Kim, A.-P. Li, and H. H. Weiering, *Nat. Mater.* **7**, 539 (2008).
- <sup>22</sup>T. George and R. Fathauer, *Appl. Phys. Lett.* **59**, 3249 (1991).
- <sup>23</sup>J. H. G. Owen, F. Bianco, S. A. Koster, D. Mazur, D. R. Bowler, and Ch. Renner, *Appl. Phys. Lett.* **97**, 093102 (2010).
- <sup>24</sup>Z. He, D. J. Smith, and P. A. Bennett, *Phys. Rev. Lett.* **93**, 256102 (2004).
- <sup>25</sup>K. Tschersich, J. Fleischhauer, and H. Schuler, *J. Appl. Phys.* **104**, 034908 (2008).
- <sup>26</sup>J. J. Boland, *Phys. Rev. Lett.* **65**, 3325 (1990).
- <sup>27</sup>P. Hohenberg *et al.* *Phys. Rev.* **136**, B864 (1964).
- <sup>28</sup>W. Kohn *et al.* *Phys. Rev.* **140**, A1133 (1965).
- <sup>29</sup>G. Kresse and J. Hafner, *Phys. Rev. B* **47**, 558 (1993).
- <sup>30</sup>G. Kresse and J. Furthmüller, *Phys. Rev. B* **54**, 11169 (1996).
- <sup>31</sup>D. Vanderbilt, *Phys. Rev. B* **41**, 7892 (1990).
- <sup>32</sup>H. J. Monkhorst and J. D. Pack, *Phys. Rev. B* **13**, 5188 (1976).
- <sup>33</sup>A. Rodriguez-Prieto and D. R. Bowler, *Phys. Rev. B* **80**, 155426 (2009).
- <sup>34</sup>A. Rodriguez-Prieto and D. R. Bowler, *J. Phys. Condens. Matter* **22**, 345001 (2010).
- <sup>35</sup>D. R. Bowler and J. H. G. Owen, *J. Phys. Condens. Matter* **14**, 6761 (2002).
- <sup>36</sup>J. H. G. Owen, K. Miki, H. Koh, H. W. Yeom, and D. R. Bowler, *Phys. Rev. Lett.* **88**, 226104 (2002).
- <sup>37</sup>O. Sakata, W. Yashiro, D. R. Bowler, A. Kitano, K. Sakamoto, and K. Miki, *Phys. Rev. B* **72**, 121407(R) (2005).
- <sup>38</sup>W. E. McMahon, I. G. Batyrev, T. Hannappel, J. M. Olson, and S. B. Zhang, *Phys. Rev. B* **74**, 033304 (2006).
- <sup>39</sup>Q. H. Wang and M. C. Hersam, *J. Am. Chem. Soc.* **130**, 12896 (2008).
- <sup>40</sup>M. C. Hersam, N. P. Guisinger, J. W. Lyding, D. S. Thompson, and J. S. Moore, *Appl. Phys. Lett.* **78**, 886 (2001).
- <sup>41</sup>F. J. Ruess, L. Oberbeck, M. Y. Simmons, K. E. J. Goh, A. R. Hamilton, T. Hallam, S. R. Schofield, N. J. Curson, and R. G. Clark, *Nano Lett.* **4**, 1969 (2004).
- <sup>42</sup>J. Wang, M. Li, and E. I. Altman, *Phys. Rev. B* **70**, 233312 (2004).
- <sup>43</sup>J. H. G. Owen and K. Miki, *Nanotechnology* **17**, 430 (2006).